Experimental assessment on machinability performance of CNT and DLC coated HSS tools for hard turning

Venkatesh Chenrayan[1,*], Chandru Manivannan[2], Selladurai Velappan[3], Kiran Shahapurkar[1], Manzoore Elahi M. Soudagar[4] , T.M. Yunus Khan[5], Ashraf Elfasakhany[6], Ravinder Kumar[7]*and Catalin I. Pruncu[8*]

[1]School of Mechanical, Chemical and Materials Engineering, Adama Science and Technology University, Adama, Ethiopia; kiranhs1588@astu.edu.et

[2]Department of Mechanical Engineering, Dhirajlal Gandhi College of Technology, Salem- 636309, Tamilnadu, India; mechchandru123@gmail.com

[3]Department of Mechanical Engineering, Coimbatore Institute of Technology, Coimbatore- 641014, Tamilnadu, India;selladurai.v@gmail.com

[4]Department of Mechanical Engineering, Glocal University, Delhi-YamunotriMarg, SH-57, Mirzapur Pole, Saharanpur District, Uttar Pradesh-247121, India; me.soudagar@gmail.com

[5]Department of Mechanical Engineering, College of Engineering, King Khalid University, Abha 61421. Kingdom of Saudi Arabia; yunus.tatagar@gmail.com

[6]Mechanical Engineering Department, College of Engineering, Taif University, P.O. Box 11099, Taif 21944, Saudi Arabia; ashr12000@yahoo.com

[7]Department of Mechanical Engineering, Lovely Professional University, Phagwara, 144411, Punjab, India; Email: rav.chauhan@yahoo.co.in

[8]Design, Manufacturing & Engineering Management, University of Strathclyde, Glasgow, G1 1XJ, Scotland, UK

[*]Corresponding author email: rav.chauhan@yahoo.co.in; Catalin.pruncu@strath.ac.uk

Abstract: The present work investigates the deposition of carbon nanotubes (CNT) over the HSS tool. Also, it assesses the machining capacity of the coated tool with respect to some of most important aspects of the machinability, such as surface roughness, cutting tool-tip temperature, cutting forces, tool wear, and service life. The Plasma Enhanced Chemical Vapour Deposition (PECVD) technique was used to deposit CNTs over the substrate. To recognize the dense deposition of CNTs, microstructural analysis was carried out through Scanning Electron Microscopy (SEM) and Raman spectroscopy. Further, a scratch test was embedded to validate the bonding strength of the covered layer substrate. Machining experiments were performed using CNT and Diamond-Like Carbon (DLC) coated tools. The analysis of experimental outcomes for three different cutting environments shows that the CNT coated tool represent a viable candidate for machining of harder materials. We have observed a dramatic reduction of the cutting tool tip temperature and cutting forces due to the excellent mechanical and thermal properties of CNTs. Indeed, the CNT coated tools prove their

suitability when compared with the DLC coated tools. The analysis of tool wear demonstrated a much lower wear condition for CNTs tools when comparing to DLC coating one. This was translated in longer tool life for the CNT coated tool, which was about 28 minutes longer with only marginal failure under high cutting conditions when comparing to DLC one.

Keywords: Carbon nanotube (CNT); Diamond-Like Carbon (DLC); coating; cutting tooltip temperature; cutting forces; scratch test; Tool wear

1. Introduction

The most common method of DLC deposition is Plasma Enhanced Chemical Vapour Deposition (PECVD). The recent challenges in the machining industry are the consumption of cutting fluids, tool wear, etc., which are inevitable when processing advanced materials. Hard turning is typically performed without coolant, which reduces production costs and offers an ecological benefit. But a major difficulty in dry machining at high temperatures is related to extensive wear of tools. Various tool coatings, such as titanium nitride (TiN), titaniumaluminium nitride (TiAlN), Chromium nitride (CrN2), etc., are widely used nowadays to minimize tool wear and thereby improve the working life of cutting tools.

High speed steel (HSS) tool is readily available and cost-effective, and therefore many small scale industries still use the HSS tool for the machining of various workpieces. HSS Tool is more resistant to heat and wear than high carbon steel. The use of various coatings on the HSS tool substrates further enhance the wear resistance property, improve tool life with reduction of wear, and enable the machining of tougher materials. By applying carbon coatings like CNT, DLC, etc., on HSS tools, whose performance competes with that of more advanced coated tools, is possible achieving a reasonable cost. The development of the cutting tool with minimal wear is of extreme urgency to reduce tool costs over the cost of production.

Properties such as high hardness, low friction, and thermal expansion coefficients draw further attention from Diamond-like carbon (DLC) coatings. The DLC coatings produced by PECVD contain a huge amount of hydrogen (40-60%). Therefore, they usually are recognized as simple a-C: H or hydrogenated diamond-like amorphous carbon film. They genenrally combines metastable sp^2 and up to 70% sp^3 high fraction carbon bonding[1]. R. Giovanni dos Santos et al. [2] have experimented DLC coated cemented carbide inserts to evaluate the machining forces during the turning of Al-Si alloys (12 wt. % and 16 wt. % of Si). The author recognized that the use of DLC deposited tools reduces feeding forces when Al-Si alloys are turned. Few researchers explored the performance of DLC coated cutting tools on different workpiece materials under various cutting operations and and it was observed a much reduced process of adhesion for the DLC layer over the substrates [3-9]. These authors found that during machining of aluminium alloys,

DLC films allows to avoid the adherence of aluminium on the tool surface, reduce cutting forces, increase the surface roughness and accuracy of the machined surface, facilitate the evacuation of chips and reduce the wear significantly. In some situations, the usage of composite coatings is more advantageous than the single-layer coatings as their combined constituents generate an unique property. The tool wear and surface roughness of three different types of DLC coated, DLC/(Al, Cr)N coated, and uncoated HSS tools were examined by Tadahiro Wada et al. [10] for turning Al with 2% and 4% Si alloys. These authors has found that DLC with a Cr-based inter-layer demonstrated less wear progression and lower surface roughness for a certain cutting length than DLC coated tool. T.C.S.Vandevelde et al. [11] examined the performance of various coatings, namely DLC, amorphous hard carbon (HC), and Diamond coatings over WC-Co inserts for Al-SiC metal matrix composites in dry turning. The outcome of the experiment showed that the CVD diamond-coated inserts faciliate a longer life than the other two types. H. Hanyu et al. [12] developed a smooth surface of finely crystallized diamond coating by applying DLC coating over CVD diamond coating on cutting tools. This coating demonstrated superior qualities of both, lubricity and durability, which leads to improvement in the anti-sticking capability of cutting tools against aluminium alloy, and longer tool endurance. Mingjiang Dai et al. [13] analyzed the cutting performance of diamond and DLC coated cemented carbide inserts against uncoated one when cutting of Al-22% wt. Si alloy, mid-Si-Al alloy, and abrasive aluminium bronze. Their results revealed that while cutting middle abrasive materials, DLC coated insert has seven times longer wear life and while manchining mid-Si-Al alloy enable 1½ times longer wear life than the uncoated one.

Carbon nanotubes are cylindrical molecules formed by rolling up single-layer carbon atoms graphene sheets. The CNT structure consists of extremely strong interactions of sp^2 bonds. In recent times, the use of carbon nanotubes is becoming significant in the development of hard surface coating due to their excellent tensile and shear strength, self-lubricating properties, high thermal conductivity, wear resistance, and low friction coefficients [14]. Pazhanivel et al. [15] performed an experiment to study the wear, and machinability properties of CNT coated inserts. They concluded that a significant decrease in the coefficient of friction of the MWCNT coated inserts resulted in improved machinability with a better surface finish. Atsushi Hirata et al. [16] studied the sliding friction properties of CNTs on substrates of silicon, cemented carbide, and silicon nitride. The findings showed that the CNTs coated substrate had better lubrication and a higher adhesive strength on surface porosity substrates. CNT coatings achieved a dramatically improvement on the wear resistance than the pure nickel coatings developed through pulsed electrode deposition [17,18]. J.P. Salvetat et al. [19] studied the mechanical properties of single and multi-walled carbon nanotubes. The structure of the nanotubes due to the high anisotropy of graphite strongly influences the mechanical characteristics. The Young's modulus of small SWCNTs is higher than graphite. The degree of order in the tube walls firmly influences the Young's modulus of the MWCNTs.

A property that measures the stiffness of the film is Young's modulus. Young's modulus of CNT coating is more than 1 TPa [19,20] which is much higher than DLC's which is only 100-300 GPa [1]. The mechanical and corrosion properties of CNTs coated mild steel were investigated by Mahmud Abdulmalik Abdulrahaman et al. [21] at different coating conditions, such as specific temperature, hold time, etc. They noted that the increased coating temperature and holding time increases tensile strength, yield strength, and hardness of mild steel coated samples and reduces the corrosion rate. Various authors investigated the single and multilayered composites carbon nanotube coatings on a variety of substrates in order to improve the mechanical, thermal and anti-corrosive properties [22-26].Properties such as poor thermal conductivity, retention of hardness even at high temperatures, and chemical reactivity are key factors making titanium alloy as a material of low machinability [27].

Most of the existing research literature deals with carbide tools as substrate which is mainly coated with titanium and chromium composite components. In this research work, the novel and unique SWCNTs coating were attempted to deposit through PECVD method, over a widely used HSS cutting tools. The workpiece considered for machining in this work is a low-machinability material titanium alloy. Here we proposed a novel approach to improve the quality of machining attributes by retaining the tool life. This unique coating is intended to cover the gap between dry machining and low machinability. Further, we have noted that CNT deposition over the HSS tool and performance evaluation of all machining attributes in a single work was not reported before. To further endorse the CNT benefits, we evaluated its properties and performance against the widely used DLC coated tool.

2. Materials and Methods

2.1. CNT Coating procedure

Carbon NanoTubes (CNT) were grown by Plasma Enhanced Chemical Vapour Deposition (PECVD) system (Roth and Rau microsystems, HBS 500, Germany). Initially, the substrate used for CNTs deposition was thoroughly cleaned using an ultrasonic cleaner for 20 min. This was made in order to achieve a free surface of dirt, dust, and foreign particles. Then, right before of CNTs deposition we have applied a thin film of Nickel on the HSS substrate. It has the catalyst role on the DC sputtering technique in order to grow the CNTs. A gaseous mixture of methane and hydrogen was employed to deposit Single-Walled Carbon Nano Tubes (SWCNT) by the PECVD apparatus. **Table 1** depicts the coating conditions applied for the deposition of the CNTs under various bias voltages ranging from 200 to 400 V and 200 W microwave powers. A gaseous mixture of methane and hydrogen is indicated to reach the maximum flow for about 50 min in order to deposit a larger diameter of CNTs [28].

Table 1. Coating conditions.

Flow rate for methane	3 cc/min

Flow rate for hydrogen	20 cc/min
Microwave power	200 W
Pressure	2.99 x 10^2 Pa
Bias voltage	200-400 V
Deposition time	50 min

2.2. Coating characterization

The surface morphology of CNT coating was studied using a Carl Zeiss Sigma field-emission scanning electron microscope. HORIBA LabRAM HR Evolution spectrometer was used to obtain the micro-Raman spectrum of CNT coated on the HSS substrate. It was achieved under a backscattering geometry of 532 nm excitation wavelength. The assessment of coating adherence was performed under a DUCOM micro scratch tester, in which a 0.2 mm diamond stylus was moved over a coated specimen surface for a stroke length of 6 mm with a traction speed of 0.2 mm/s. The ramp load was settled as linearly increasing order, 20 N at the beginning and 45 N at the end. This later test was carried out until failure occurred at critical loads. With the help of an optical microscope, the scratch was analyzed, and the value of the width of track caused by the indenter was revealed.

2.3 Turning experiments

FLIR E50 thermal image camera was employed to measure the temperature at cutting zone during turning process of titanium alloy workpiece having a diameter of 50 mm and length of 150 mm, respectively. The thermal image camera was equipped with an auto orientation facility, 3.1 MP IR resolution (240 x 180), frame refresh of 60 Hz, and 0.05 °C thermal sensitivity. It has a recording capacity between minimum -20 °C to a maximum of 1000 °C, which was fixed over a special fixture as shown in **Figure 1**. The constant contact proximity was achieved by setting accurate angle and height adjustments available in the fixture, which enabled the movement over the tool carriage.

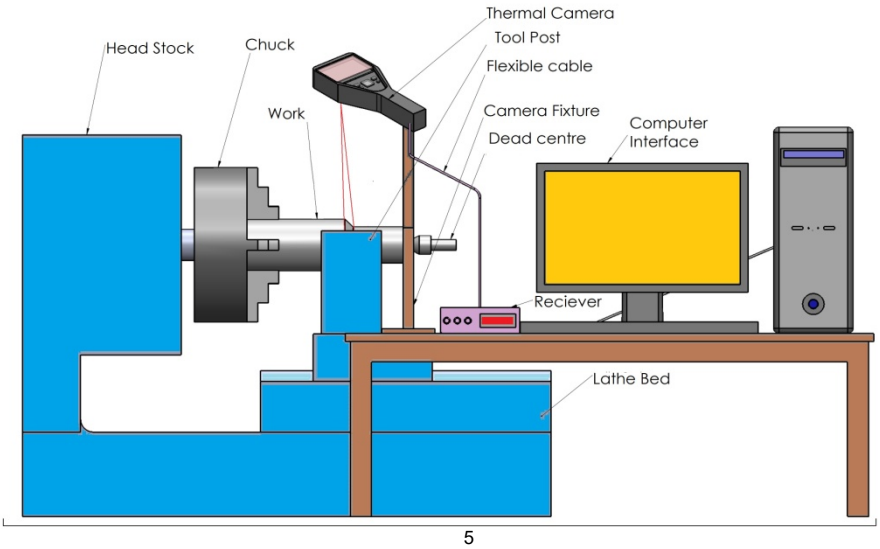

Figure 1. Schematic arrangement of the infrared thermal image camera.

The arithmetic mean surface roughness (R_a) represents the average surface peaks and valleys of the workpiece surface evaluated.It was measured by using MITUTOYO SJ 410 surface roughness tester. To measure the wear growth for all cutting conditions, an Atomic Force Microscope (NTEGRA, NTMDT, Russia) and DINO-LITE digital Microscope with a resolution of 640 x 480 pixels, magnification range of 10 x to 230 x, and frame rateof 30 FPS was employed. A commercialgrade 5 titanium alloy was used as a working material for machining experiments. The chemical composition and mechanical properties were shown in **Table 2** and **Table 3**, respectively.

Table 2. Chemical composition of titanium alloy Grade 5.

Chemicals	O	V	N	H	Al	Fe	C	Ti
Percentage	0.2	3.5- 4.5	0.05	0.0125	5.5- 6.75	0.4	0.1	Balance

Table 3. Mechanical properties of titanium alloy Grade 5.

Hardness	Tensile strength (MPa)	Yield strength (MPa)	Reduction of area in %	Elongation in %
RC36	895	825	25	10

Table 4. Specifications of the turning apparatus.

CNC system	Fanuc 0i-Mate TD
No. of Axis	2
Turret capacity	8 Tools
X-axis	140 mm
Z-Axis	400 mm
Max Spindle speed	3000 rpm
Distance between centers	425 mm
Max. turning diameter	270 mm
Max. turning length	400 mm

The turning experiments were carried out under a CNC lathe (Jobber LM, ACE micromatic) as per specification made in **Table 4**. The machining parameters chosen for the experiment are shown in **Table 5**.

For the experiments, two distinct types of coated HSS tools (CNT and DLC) were used. DLC was deposited over the HSS tool at Central Manufacturing Technology Institute, Bengaluru, India, through the state-of-the-art PECVD equipment.

Table 5. Machining parameters.

Level / Parameter	Level 1	Level 2	Level 3
Cutting Speed (m/min)	250	350	450
Feed rate (mm/rev)	0.2	0.25	0.3
Depth of cut (mm)	0.3	0.5	0.8

3. Results and Discussion

3.1. Characterization of CNT deposition

Figure 2 shows the characteristics of Raman spectroscopy peaks identified on SWCNTs surface. While the CNT was breathing during the deposition process, the C atoms were subjected to atomic vibrations in the radial direction, which was detected by the Radial breathing mode (RBM) feature of Raman. The RBM confirmed the presence of SWCNT with a diameter range between 50 nm - 60 nm (see details in **Figure 3**); otherwise, the RBM was not detected in CNTs. Moreover, the G band, which represents the Raman – allowed a tangential mode in HSS and it was observed at 1582 cm^{-1}that endorses the signature of CNTs [29]. The G band around 1580 cm-1 experienced a splitting (G^+ and G^- peaks), which is an indication of anisotropic in-plane C-C stretching mode due to the curvature of the nanotube. Besides, a weak D band around 1350 cm^{-1} suggests that the SWCNT used in this study is of high structural quality.

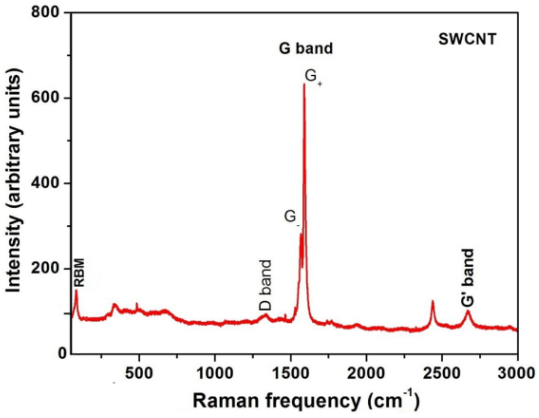

Figure 2. Patterns of Raman Spectroscopy of the CNT film.

Clear images of coated carbon nanotubes with smaller aspect ratios were depicted in **Figure 3**. The SEM images confirm that the CNTs deposited are densely over the substrate. In literature, there were some attempts [30] to investigate adherence quality of CNT coatings on the substrate. They observed that the

lengthy CNTs were frequently and easily pulled away from substrates, which pose difficulties to detect their adherence. Generally, the adherence of the coating with the substrate is inversely proportional to the aspect ratio (Length/Diameter) of CNTs, and hence, in order to achieve a better adhesion, the CNTs should possess a smaller aspect ratio [15]. The length of the CNTs deposition can be controlled by varying the microwave power of the PECVD [16].

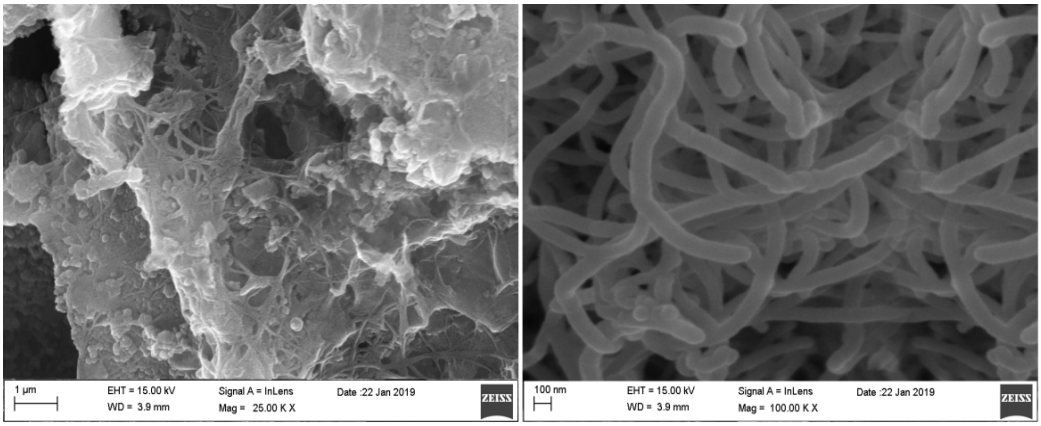

Figure 3. Patterns of SEM images of CNT deposition.

3.2 Adhesive strength of the CNT deposition

Figure 4 depicts the scratch test results. In this figure we have plotted four different curves in order to better understand the physical mechanism. There, the black line expresses the evolution of coefficient of friction while the green line represents the acoustic emission. Normal load and traction force are represented by the rest of the two lines, red and blue, respectively. The average value of the coefficient of friction associated to CNT film deposited over the HSS substrate was about 0.075. There it was noted 3 different behaviour for the friction coefficients. The first run part of friction coefficient was up to 0.9 mm, which showed a COF about 0.05 with some small fluctuation. Then we have noted a steady state increase of COF up to 0.07 for a stroke length about 2.6mm. The last part shows initially a steady state friction coefficient for about 1 mm followed by two different rapid increase of the COF. Similar results for the coefficient of friction of CNT deposition over the WC inserts were reported by Atsushi Hirata et al. [16]. The scratch measured by the optical microscope indicated width of 123 µm. Otherwise, the Acoustic Emission signal followed an exponential increase with the maximum of 0.11.

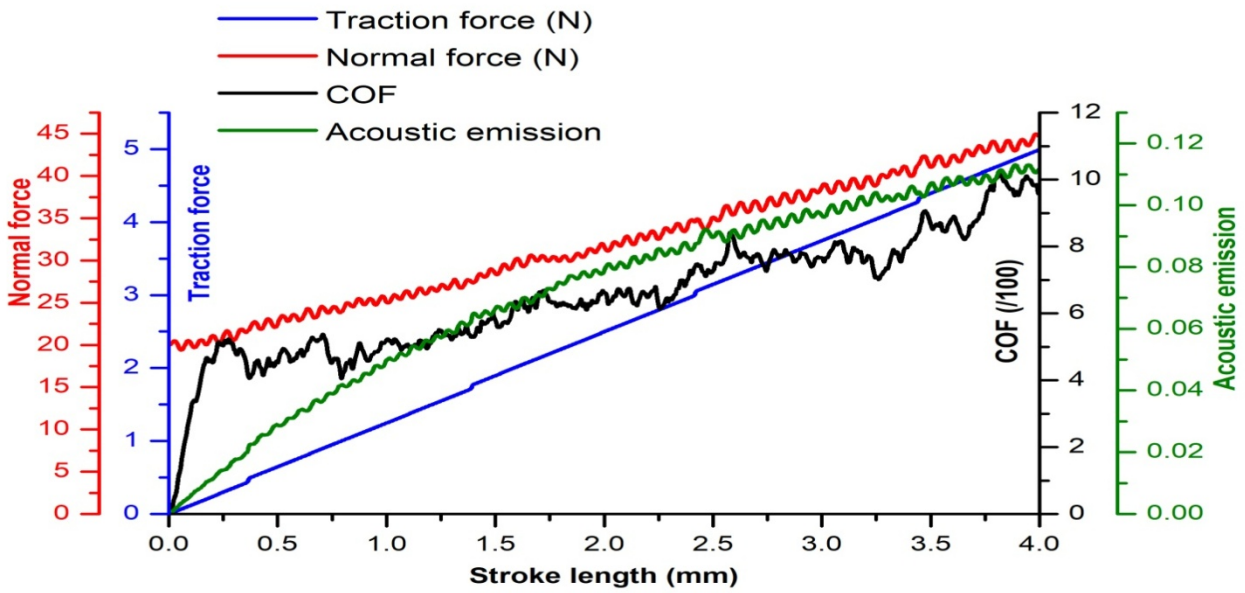

Figure 4. Scratch test result exhibiting the traction and normal force, friction coefficient and acoustic emission, related to the HSS steel covered by CNT.

The mathematical value of adhesion strength of the coating with the substrate material was found by using the following Equation (1).

$$\sigma_A = \frac{2W_C}{\pi R b} \quad (1)$$

Where,

σ_A – adhesion strength (N/mm^2)

R – Radius of stylus point (mm):0.2 mm

W_C – Detected critical load (N): 26N

b – Width of the track caused by indenter (mm): 123 µm

The adhesion stress evaluated by the above relationship is 673 N/mm^2, which is almost 3/4th of its yield strength that is nearly 900 N/mm^2.

3.3 Cutting tool temperature

The performance of the cutting tool can be significantly affected by the development of cutting temperature at the cutting tool-tip and workpiece interface. Three different cutting conditions were used to observe the performance evolution of DLC and CNT coated tools. The temperature results recorded from the infrared image for both DLC and CNT coated tools imposing level 1 of cutting condition are shown in **Figure 5**. The Figure 5 (a) indicated that the maximum temperature recorded for DLC coated tool was 152.7 °C whereas in Figure 5 (b) are depicted the temperature value for CNT coated tool which is 97.8 °C. The color region yellow expresses the maximum temperature and bluish region expresses the minimum temperature. The rectangular box (bounding box) represents the target region of tool and work piece interface.

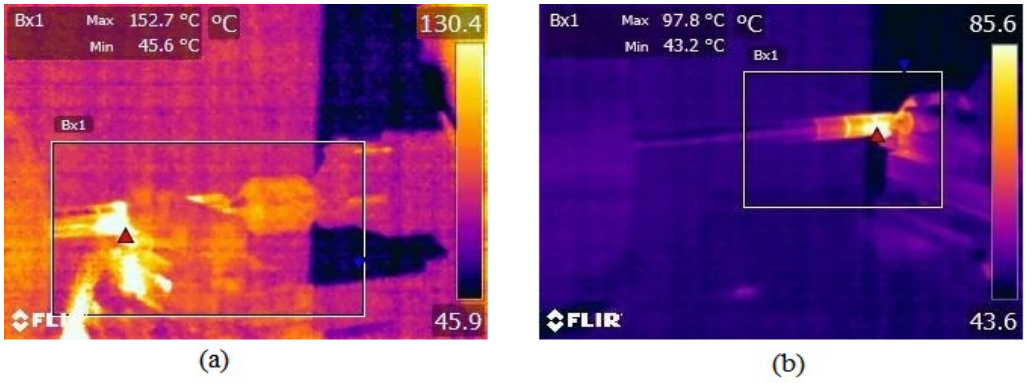

Figure 5. Infrared thermal images captured during machining with (a) DLC coated tool and (b) CNT coated tool imposing Level 1 cutting condition.

The results plotted in **Figure 6** endorses the fact that the cutting tool temperature increases with cutting speed for both DLC and CNT coated tools, respectively. However, the increment in temperature for the DLC coated tool is higher than that of the CNT coated one. The comparative temperature was recorded for a constant cutting time of 15 minutes for all machining conditions. From the graphs in Figure 6, it is evident that the cutting tip temperature of the CNT coated tool reveals lower temperatures which are nearly 30 % to 35 % lesser in comparison with the DLC coated tool under all three levels of the cutting conditions.

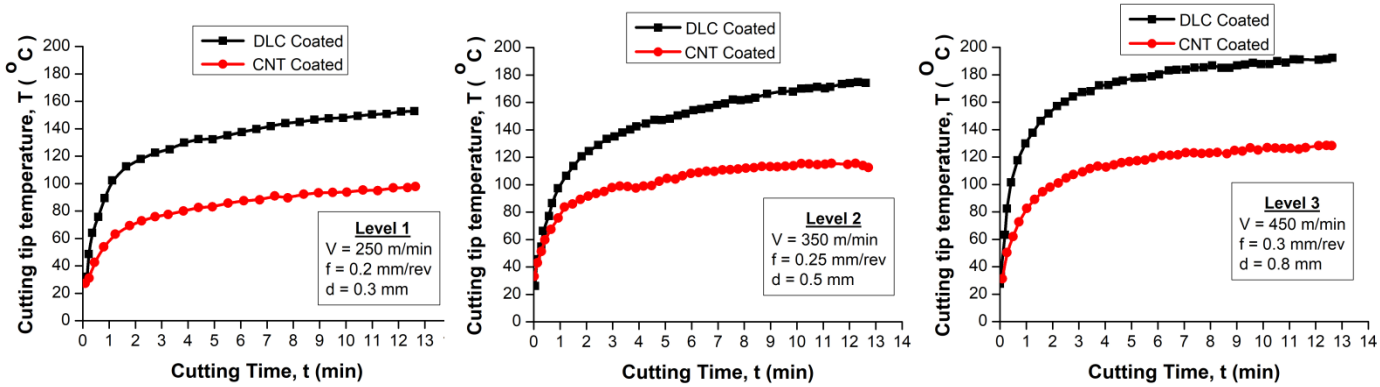

Figure 6. Temperature results for (a) Level 1 (b) Level 2 (c) Level 3 cutting conditions.

A significant increment in thermal conductivity was observed for very low sp^2 bond contents in the graphitic region [31]. Since CNT consists of a large quantity of low sp^2 bonds, its thermal conductivity is in the range of 4000-6000 W/mK [20], which is superior to that of DLC (0.566 W/mK) [31]. This noble quality of CNT helps to drain out the majority of heat developed at tool and workpiece junction to the environment through chips. The exceptional tribological and excellent thermal conductivity of CNTs result in a considerable reduction of tool-tip temperature while machining. Normally the contact between tool-tip and workpiece induces greater friction that lead to heat generation. The noticeable difference in friction coefficients of DLC and CNT permits to explain the difference in temperature effect. The CNT coated tool revealed an average coefficient of friction of about 0.075 resulted from the scratch test. Yet, some previous research [32, 33] reported a slightly higher coefficient of friction for DLC coating in range of 0.17 to 0.25. This much lower value of friction coefficient associated to CNT tool can be considered responsible for lower heat generation at

the tool-tip/workpiece interface. We speculated that when the coefficient of friction is low probably the abrasion between the chip and tool induces the sliding effect, which in turn can minimize the contact heat due to reduced frictional effect. The superior thermal conductivity of the CNT coating also helps to minimize the tool tip temperature owing to its higher heat dissipation rate. Thus, the combined effect of low frictional co-efficient and higher thermal conductivity of the CNT coated tool works as a barrier for heat dissipation and the cutting tool tip temperature remain at a lower level. Jingjie et al. [34] reported that the TiAlN coated tool demonstrated nearly 60 % reduction in cutting tool tip temperature owing to its better anti-friction property.

3.4 Cutting forces

The machinability performance of the tool is greatly influenced by the induced cutting forces exerted over the tool while machining. The cutting forces were evaluated by using a combined "KISTLER 5697A" dynamometer and data acquisition program DynoWare. The cutting and feeding forces were measured for DLC and CNT coated cutting tools for three levels of cutting conditions by performing cutting opertaion for 60 seconds for each trial. **Figure 7** shows the results details for a sample subjected to Level 1 cutting condition using the dynamometer and the DLC coated tool. Further, in **Figure 8** were depicted the comparative results of cutting forces for both DLC and CNT coated tools under all cutting conditions. From these graphs, we have noted that the tangential forces (F_z) exerted over the CNT coated tool subjected to three different levvel of cutting conditions is reduced by almost 35.9% when compared with DLC coated tool. Similarly, the feed forces (F_y) for CNT coated tools is reduced by the almost 47.7%, and the radial forces (F_x) is reduced by almost 54% in comparison with the DLC coated tool, respectivly.

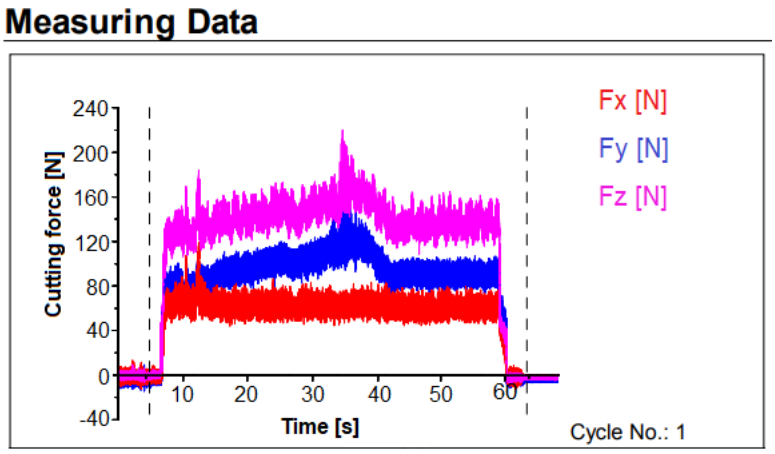

Figure 7. Sample Dynamometer observation for DLC coated tool at Level 1 cutting condition.

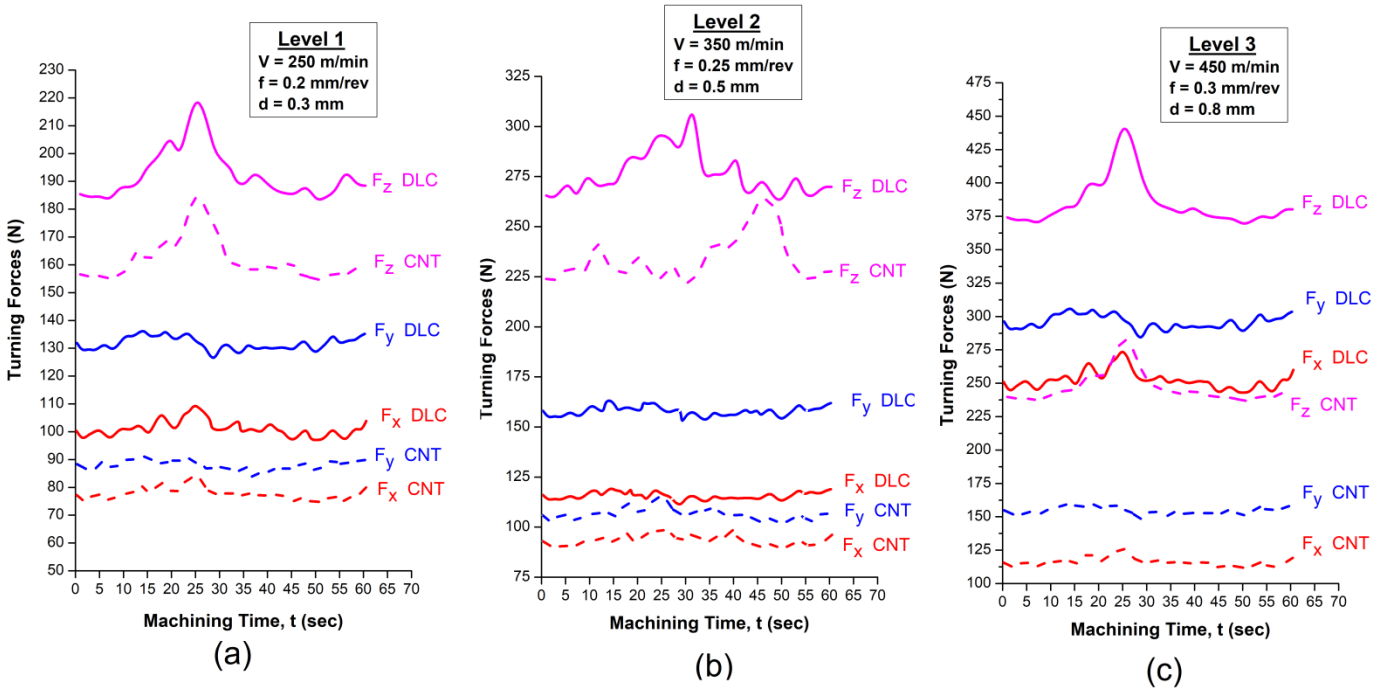

Figure 8. Results of cutting forces for different level conditions: (a) Level 1 (b) Level 2 (c) Level 3 cutting conditions.

The graphs from Figure 8 indicated that the cutting forces from DLC coated tool trigger sligtly high increment in cutting forces at high cutting speed and depth of cut. This is probably due to the formation of a build-up edge at elevated temperature. Moreover, the CNT coatings are capable to achieve betterlubricity under various test conditions [14]. The radical reduction of cutting forces in the CNT coated tool is attributed to the excellent lubricity or anti-friction effect of the CNT coated surface which is denoted by very low coefficient of friction. Another important factor that influences the depletion of cutting forces is the high thermal conductivity of CNTs is asscociated to the thermomechanical effect. In this case, the majority of the heat is carried away by the chip and work material. Therefore, the high thermal conductivity of CNTs is resposnable for dissipating of excessive heat from the cutting tool and probably the work material obey an uniform plastic state. The pre yielded work material ensures the machining with miniumum effort.

3.5 Surface roughness

Surface roughness is the most predominant feature in estimating the machined components of surface quality. For each experiment, we have taken the readings at three different locations around the

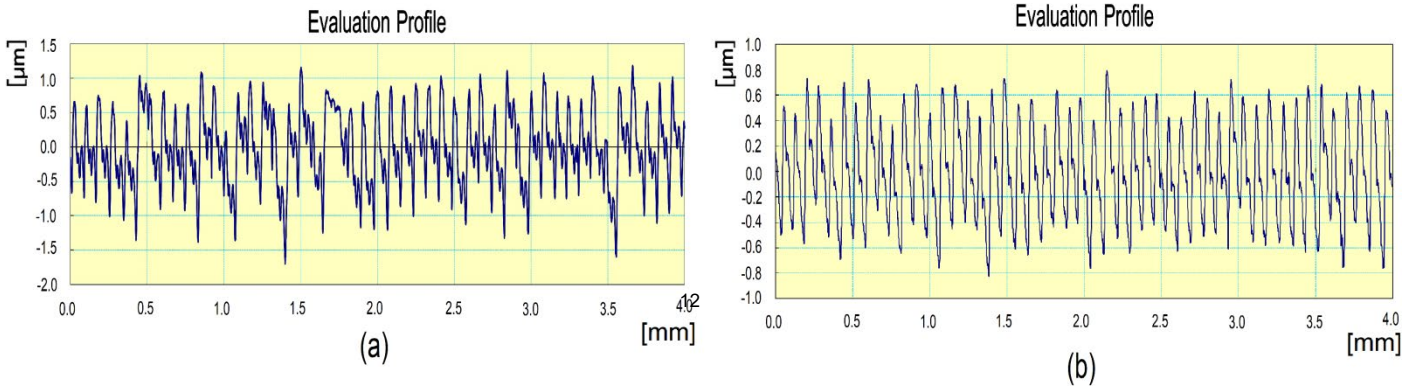

circumference of the work material at 120° and maintaining a trace length of 4mm. **Figure 9 (a) and (b)** show the sample observations obtained from the surface roughness tester for DLC and CNT coated tools, respectively. The comparative average surface roughness value recorded for both DLC and CNT coated tools at each trial is shown in **Figure 10**.

Figure 9. Sample Surface roughness image for (a) DLC (b) CNT coated tools

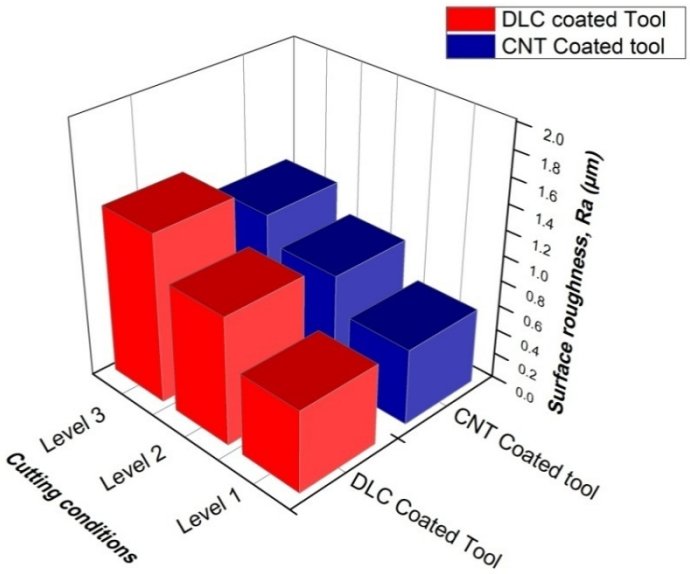

Figure 10. Comparative surface roughness results.

Generally, the vibrations that occurred during the machining process can be decomposed into three directions, namely radial, longitudinal, and circumferential. Here, the vibration in radial direction can severely affects the peak of the surface roughness. Moreover, we have noted that the surface coating does not have any significant impact over this vibration, that is why both the tool records more or less the same average surface roughness value for all three cutting speeds. **Figure 10** confirms that the surface roughness of the workpice machined with CNT coated tool under three cutting conditions was reduced by almost 19% when compared with that of the DLC coated tool. The magnitude of nose wear for the CNT coated tool was very less owing to its anti-friction property, which minimizes the surface roughness to a maximum extent.

3.6 Tool life and wear mechanisms

The wear process on the cutting tool do not affects only the tool life but it has also impact on the product cost. This explain why research comunity and industry are tring to solve and improve the tool surface. Therefore, it gained major importance whenever the machinability aspect of the cutting tool is concerned. **Figure 11(a) and (b)** illustrate the sample images captured through AFM for the DLC and CNT coated tools subjected to level 3 cutting condition, respectively. The demaged tool surface is related to proeminence of peak and valleys located in the surafces acquired by AFM images. Indeed, these peaks and valleys captured through AFM images replicate the worn out tool surface.Various researchers [35] confirmed that the increase on the cutting speed will generate accentuated peaks and valleys which are sign of tool life deterioration with

directly impact on the work piece. There the loss of tool life can be ascribed as a function of cutting temperature.

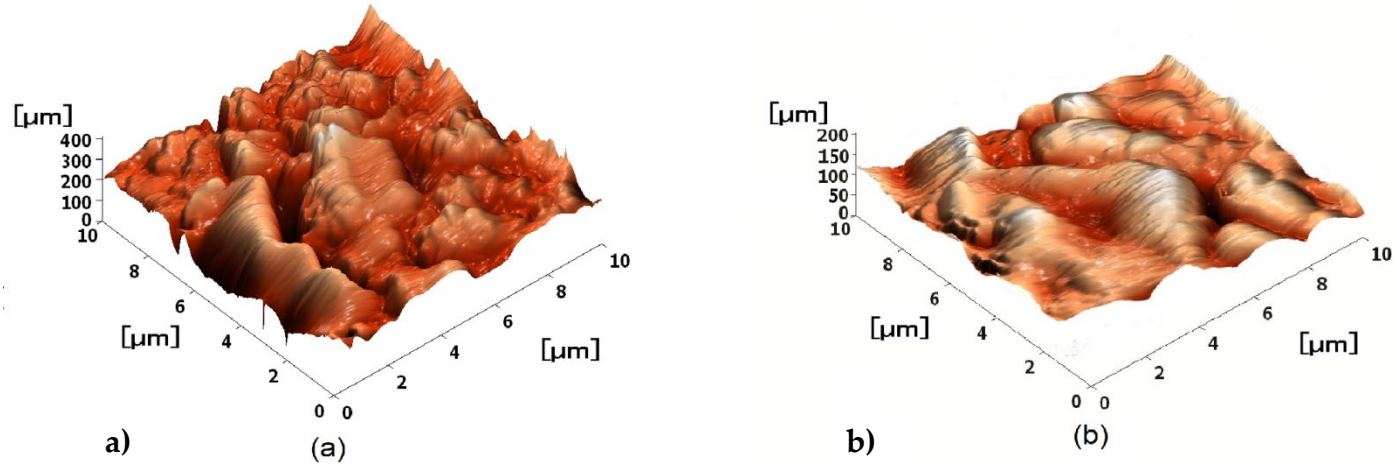

Figure 11. Sample AFM images of flank wear observed for a) DLC and b) CNT coated tools subjected to level 3 conditions

Figure 12 displays the progress of flank wear of both tools under three different cutting conditions. In these images we can noted that the CNT-coated tool reveals much lower wear in contrast to DLC-coated one. The reduction in the flank wear rate for CNT-coated tool is almost 20 to 25% compared to the DLC-coated tool.

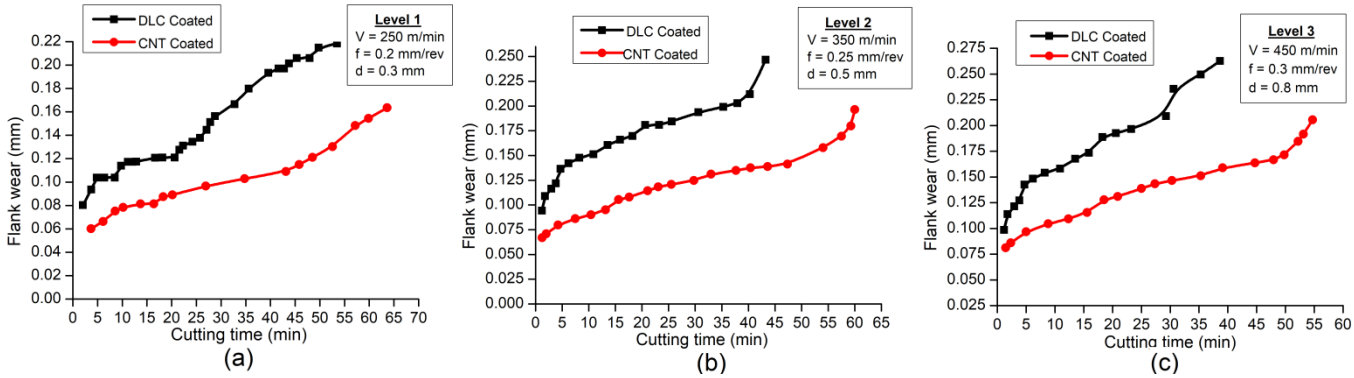

Figure 12. Flank wears results (a) Level 1 (b) Level 2 (c) Level 3 of cutting conditions.

Also we have noted from Figure 12 that the DLC coated tool failed much early i.e. at 53, 43, and 39 minutes in catastrophic failure mode under the three different cutting conditions studied (see details In Figure 12 (a), (b) and (c)). Moreover, when was used the CNT-coated tool the failure was achieved at around 65 minues for Level 1 and level 2 and 55 minutes for Level 3. The wear rate of DLC film may increase rapidly when the tempaerture change from room temperature to almost 200 °C and/or above. Further, this drastic increase on tempearture is leading to rapid worn out of DLC structure and complete rupture of coating [36]. The growth of wear is directed proportial with the increase in the cutting parameters, therefore it trigger massive material loss as we can observe at the flank portion of the DLC coated tool (see details in **Figure 13)**.

At high temperature the tool material becomes plastic. Therefore, when the abrasion action take place between tool and chip,the plastic condition accelerates the material loss from the tool. Neverthless, the minimum loss of material was recored on the CNT coated tool. This could be also due to its low frictional coefficient of CNTthat promote negligible effect on abrasion.

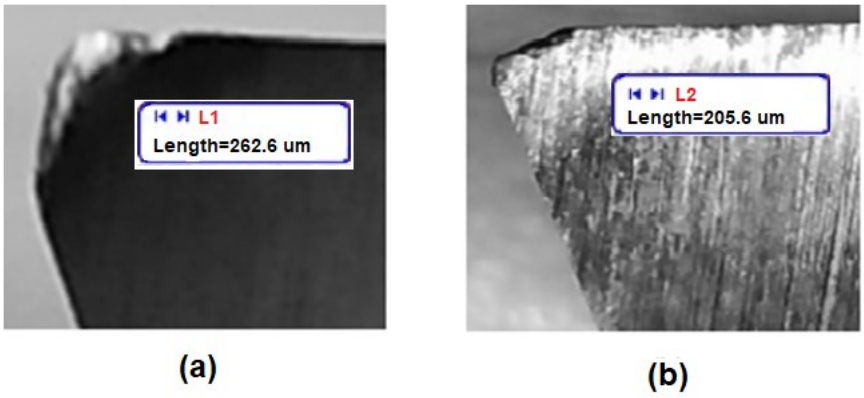

Figure 13. Flank wear images of (a) DLC (b) CNT coated cutting tools after the catastrophic failure.

A comparative lifetime of both DLC and CNT coated tools was shown in **Figure 14** under three different cutting conditions. Test results indicate that the CNT coated tool has a much longer tool life than that of the DLC coated tool. It is more than 16 minutes longer when is used extreme cutting. In particular, the CNT coated tool worked much better under severe cutting conditions (high cutting speed, high depth of cut associated to Level 3) without significant failure.

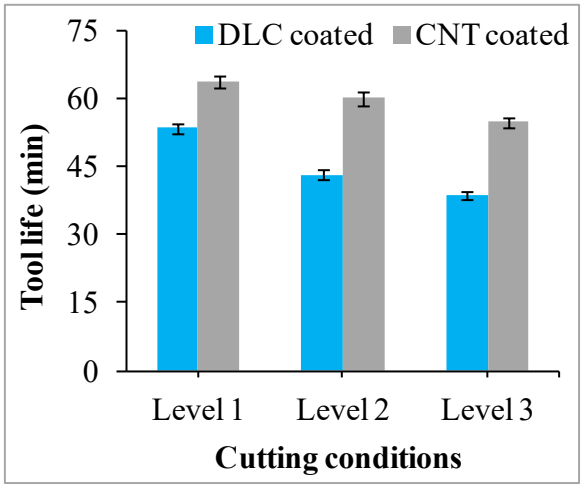

Figure 14. Tool life comparison of both tools for three different cutting conditions.

Figure 15 displays the effects of DLC and CNT coated tools for nose wear. The results depict a serious growth in the wear on the DLC coated tool. The cumulative impact of extreme plastic deformation and crater wear on the rake surface can be responsible for this disproportionate loss in tool life for the DLC coated tool. High compression stresses and high temperatures which are produced during the machining process can cause the tool to thermally soften, which in turn results in plastic deformation of the cutting edges. The increased

temperatures corroborated with harder level of cutting can have much detrimental effects on the cutting tool surface.

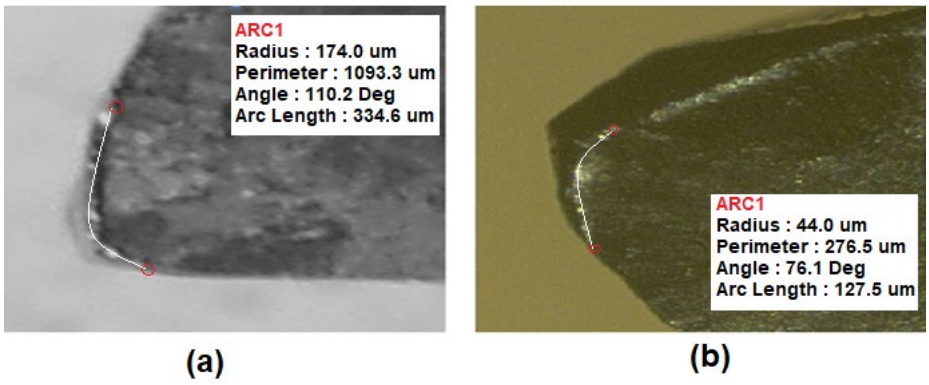

Figure 15. Nose wear images of (a) DLC (b) CNT coated cutting tools after the catastrophic failure.

Otherwise, we speculate that the low frictional coefficient and high elastic modulus properties of the CNTs are the main responsible to minimize the contact heat and compressive stresses, respectively. The lower temperature and smaller cutting forces restricts the tool to behave plastic, which in turn prevents the tool failure considerably. This combined impact motivates an increase of tool life by almost 42 % compared to DLC coated subjected to level 3 condition which are the extreme cutting environment in this study. The lowest friction coefficient of CNTs was responsible to mitigate the risk of abrasive wear which was found as minimum on the CNTs coated tools. Indeed, the chip abrasion was dictated by the surface coating anti-friction property.

Even the CNTs coated tool performed better than DLC coated one, in terms of tool life. However, specific erosion on the coating tool by CNTs was observed through optical microscope (see details in **Figure 16)**. The erosion identified on the rake surface of the coated tool especially occurred at elevated cutting conditions is attributed to the inhomogeneous distribution of CNTs over the rake surface. The inhomogeneous or less dense CNTs deposition can be susceptible to early failure, therefore, when tougher cutting condition were implemented an accelerated crater wear was produced.

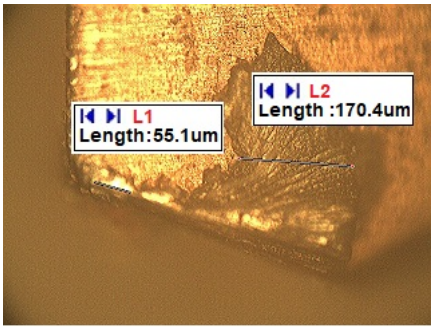

Figure16. Optical microscopic view of the CNT coated tool after turning.

4. Conclusions

In this comprehensive experimental work, the novel carbon nanotubes were deposited over the HSS tool to resolve the challenge imposed by the machinability of titanium alloy. To further validate the machinability performance of the CNT coated tool we have used the DLC coated tool as target. Three different cutting conditions were applied in order to demonstrate these coatings benefits in four key aspects, namely cutting forces, cutting tip temperature, surface roughness of the machined parts and tool wear life. The following conclusions were drawn:

1. CNTs deposited using the PECVD technique have a good substrate adhesion strength. The scratch tests demonstrated that the adhesive stress value is nearly 3/4th of the yield strength of the substrate material. The scratch test also confirms the extraordinary anti-friction behavior of the coated surface with a very low frictional coefficient of 0.075.

2. A thermal infrared imager was used to capture the cutting tip temperature produced at the tool and workpiece interface. The implementation of a CNT coating allowed a reduction of almost 35% of heat compared to a DLC coated tool. Most notably, the metal cutting capacity of the coated tool was excellent in terms of the subsidized temperature of the cutting tip at extreme cutting conditions.

3. The investigation of major cutting forces under different cutting conditions indicated that a significant depletion of cutting forces for the CNT coated tool which was recorded in the range of 12 to 54 %. The magnitude of the tangential cutting force was observed in all machining conditions to be larger than the rest of the two other forces, namely, feed force and radial force.

4. The results of surface roughness have showed that the coating does not affect much the surface roughness regardless of cutting conditions imposed. However, substantial improvement in surface roughness was achieved using CNTs coatings, about 19% by imposing high cutting conditions. The magnitude of surface texture, the peaks and valleys was noted as higher, when imposing elevated cutting conditions for both CNT and DLC coated tools.

5. The wear and life of the tools investigated by AFM and optical microscopes indicated that the CNT coated tools have longer tool life, around 55 minutes even when were used difficult cutting conditions. The flank wear on the CNT coated tool was reduced to 20 to 25% in all cutting conditions as compared to the DLC coated tool. In the case of the DLC coated tool by increasing the cutting parameters we have observed a rapid growth rate of flank wear, whereas the CNT coated tool showed a constant and slow wear trend for the same environment. Further, the tool life coated by DLC showed catastrophic failures for all three different cutting conditions at approximately 53, 43, and 38 minutes, respectively. Moreover, the CNT-coated tool was much less damaged even under higher cutting conditions and showed longer integrity for about 55 minutes.

6. The CNTs coated tool showed the erosion pattern, on a specific portion, on the rake surface for just one tested sample due to lack of homogeneity in the distribution of CNTs, which can slightly decrease the tool life.

Acknowledgments

The authors extend their appreciation to the Deanship of Scientific Research at King Khalid University, Saudi Arabia for funding this work through Research Group Program under Grant No: R.G.P 2/147/42. This work was supported by Taif University researchers supporting project number (TURSP–2020/40), Taif University, Taif, Saudi Arabia.

Conflicts of Interest: The authors declare no conflict of interest.

References

1. Erdemir, A.; Donnet, C. Tribology of Diamond-like Carbon Films: Recent Progress and Future Prospects. *J. Phys. D: Appl. Phys.***2006**, *39*, R311–R327, doi:10.1088/0022-3727/39/18/R01.
2. dos Santos, G.R.; da Costa, D.D.; Amorim, F.L.; Torres, R.D. Characterization of DLC Thin Film and Evaluation of Machining Forces Using Coated Inserts in Turning of Al–Si Alloys. *Surface and Coatings Technology***2007**, *202*, 1029–1033, doi:10.1016/j.surfcoat.2007.07.100.
3. Folea, M.; Roman, A.; Lupulescu, N.-B. An Overview of DLC Coatings on Cutting Tools Performance. *Academic journal of manufacturing engineering***2010**, *8*, 30–36.
4. Yu, G.; Gong, Z.; Jiang, B.; Wang, D.; Bai, C.; Zhang, J. Superlubricity for Hydrogenated Diamond like Carbon Induced by Thin MoS2 and DLC Layer in Moist Air. Diamond and Related Materials **2020**, 102, 107668.
5. Takeno, T.; Sugawara, T.; Miki, H.; Takagi, T. Deposition of DLC Film with Adhesive W-DLC Layer on Stainless Steel and Its Tribological Properties. Diamond and related materials **2009**, 18, 1023–1027.
6. Lu, Y.; Huang, G.; Xi, L. Tribological and Mechanical Properties of the Multi-Layer DLC Film on the Soft Copper Substrate. Diamond and Related Materials **2019**, 94, 21–27.
7. Dalibon, E.L.; Moreira, R.D.; Heim, D.; Forsich, C.; Brühl, S.P. Soft and Thick DLC Deposited on AISI 316L Stainless Steel with Nitriding as Pre-Treatment Tested in Severe Wear Conditions. Diamond and Related Materials **2020**, 106, 107881.
8. Chen, C.; Tang, W.; Li, X.; Wang, W.; Xu, C. Structure and Cutting Performance of Ti-DLC Films Prepared by Reactive Magnetron Sputtering. Diamond and Related Materials **2020**, 104, 107735.
9. Ankit, K.; Varade, A.; Reddy, N.; Dhan, S.; Chellamalai, M.; Krishna, P.; Balashanmugam, N. Synthesis of High Hardness, Low COF Diamond-like Carbon Using RF-PECVD at Room Temperature and Evaluating Its Structure Using Electron Microscopy. Diamond and Related Materials **2017**, 80, 108–112.
10. Wada, T.; Iwamoto, K.; Sugita, H. Tool Wear of Diamond-Like Carbon-Coated High-Speed Steel with a Cr-Based Interlayer in Cutting of Aluminum Alloys. *AMM***2012**, *152–154*, 74–79, doi:10.4028/www.scientific.net/AMM.152-154.74.
11. Vandevelde, T.C.S.; Vandierendonck, K.; Van Stappen, M.; Du Mong, W.; Perremans, P. Cutting Applications of DLC, Hard Carbon and Diamond Films. *Surface and Coatings Technology***1999**, *113*, 80–85, doi:10.1016/S0257-8972(98)00831-7.

12. Hanyu, H.; Kamiya, S.; Murakami, Y.; Kondoh, Y. The Improvement of Cutting Performance in Semi-Dry Condition by the Combination of DLC Coating and CVD Smooth Surface Diamond Coating. *Surface and Coatings Technology***2005**, *200*, 1137–1141, doi:10.1016/j.surfcoat.2005.02.022.
13. Dai, M.; Zhou, K.; Yuan, Z.; Ding, Q.; Fu, Z. The Cutting Performance of Diamond and DLC-Coated Cutting Tools. *Diamond and Related Materials***2000**, *9*, 1753–1757, doi:10.1016/S0925-9635(00)00296-X.
14. Zhang, W.; Ma, G.; Wu, C. Anti-Friction, Wear-Proof and Self-Lubrication Application of Carbon Nanotubes. *Rev. Adv. Mater. Sci***2014**, *36*, 75–88.
15. Pazhanivel, B.; Kumar, T.P.; Sozhan, G. Machinability and Scratch Wear Resistance of Carbon-Coated WC Inserts. *Materials Science and Engineering: B***2015**, *193*, 146–152, doi:10.1016/j.mseb.2014.12.006.
16. Hirata, A.; Yoshioka, N. Sliding Friction Properties of Carbon Nanotube Coatings Deposited by Microwave Plasma Chemical Vapor Deposition. *Tribology International***2004**, *37*, 893–898, doi:10.1016/j.triboint.2004.07.005.
17. Borkar, T.; Harimkar, S. Microstructure and Wear Behaviour of Pulse Electrodeposited Ni–CNT Composite Coatings. *Surface Engineering***2011**, *27*, 524–530, doi:10.1179/1743294410Y.0000000001.
18. Venkatesh, C.; Karthi, A.; Logeswaran, T.; Prithivirajan, V.; Santhosh, M. Experimenta l Investigation of Tribological Characteristics of Nanocrystalline Nickel Protective Coating Developed through Electro Deposition Technique. *Materials Today: Proceedings***2016**, *3*, 3121–3129.
19. Salvetat, J.-P.; Bonard, J.-M.; Thomson, N.; Kulik, A.; Forro, L.; Benoit, W.; Zuppiroli, L. Mechanical Properties of Carbon Nanotubes. *Applied Physics A***1999**, *69*, 255–260.
20. Monthioux, M. *Carbon Meta-Nanotubes: Synthesis, Properties and Applications*; John Wiley & Sons, 2011; pp. 7–36, ISBN 1-119-96094-0.
21. Abdulrahaman, M.A.; Abubakre, O.K.; Abdulkareem, S.A.; Tijani, J.O.; Aliyu, A.; Afolabi, A.S. Effect of Coating Mild Steel with CNTs on Its Mechanical Properties and Corrosion Behaviour in Acidic Medium. *Adv. Nat. Sci: Nanosci. Nanotechnol.***2017**, *8*, 015016, doi:10.1088/2043-6254/aa5cf8.
22. Tümer, D.; Güngörürler, M.; Havıtçıoğlu, H.; Arman, Y. Investigation of Effective Coating of the Ti–6Al–4V Alloy and 316L Stainless Steel with Graphene or Carbon Nanotubes with Finite Element Methods. Journal of Materials Research and Technology 2020, 9, 15880–15893.
23. Chandru, M.; Selladurai, V.; Venkatesh, C. Experimental Evaluation of Machinability Performance of CNT Coated HSS Tool during Turning of Titanium Alloy. Journal of Mechanical Science and Technology 2021, 1–10.
24. Manjunatha, K.; Giridhara, G.; Jegadeeswaran, N. Effect of Carbon Nanotube (CNT) Additions in Cr3C2-25% NiCr Coatings on Microstructural and Mechanical Properties. Materials Today: Proceedings 2020.
25. Karthick, M.; Yoganandam, K. Investigation of Mechanical Properties and Corrosion Performance of CNT Coated on EN8 Mild Steel. Materials Today: Proceedings 2021.
26. Chandru, M.; Selladurai, V.; Venkatesh, C. MultiobjectivePerforMance Investigation of CNT Coated Hss Tool under the Response Surface MetHodology Platform. Archives of Metallurgy and Materials 2021, 66.
27. Veiga, C.; Davim, J.; Loureiro, A. Review on Machinability of Titanium Alloys: The Process Perspective. *Rev. Adv. Mater. Sci***2013**, *34*, 148–164.
28. Tripathi, N.; Mishra, P.; Harsh, H.; Islam, S. Fine-Tuning Control on CNT Diameter Distribution, Length and Density Using Thermal CVD Growth at Atmospheric Pressure: An in-Depth Analysis on the Role of Flow Rate and Flow Duration of Acetylene (C 2 H 2) Gas. Applied Nanoscience 2015, 5, 19–28.

29. Jorio, A.; Pimenta, M.A.; Filho, A.G.S.; Saito, R.; Dresselhaus, G.; Dresselhaus, M.S. Characterizing Carbon Nanotube Samples with Resonance Raman Scattering. *New J. Phys.***2003**, *5*, 139–139, doi:10.1088/1367-2630/5/1/139.
30. Mangione, A.; Lanzara, G.; Torrisi, L.; Caridi, F. Mechanical Properties of Nanostructured Carbon Layers Grown by CVD and PLD Techniques. *Radiation Effects and Defects in Solids***2010**, *165*, 746–753, doi:10.1080/10420151003731652.
31. Shamsa, M.; Liu, W.L.; Balandin, A.A.; Casiraghi, C.; Milne, W.I.; Ferrari, A.C. Thermal Conductivity of Diamond-like Carbon Films. *Appl. Phys. Lett.***2006**, *89*, 161921, doi:10.1063/1.2362601.
32. C.Baucer, H.Leiste, M.Stuber, S.Ulrich, H.Holleck. Mechanical properties and performance of magnetron-sputtered graded diamond – like carbon films with and without metal addition. *Diam. Relat. Mater*. 11(2002) 1139-1142.
33. D.P.Monaghan, D.G.Teer, P.A.Logan, I.Efeoglu, R.D.Arnell. Deposition of wear resistant coatings based on diamond like carbon by unbalanced magnetron sputtering. *Surf.Coat.Technol*. 60(1993) 525- 530.
34. Zhang, J.; Liu, Z.; Du, J. Prediction of Cutting Temperature Distributions on Rake Face of Coated Cutting Tools. *Int J AdvManufTechnol***2017**, *91*, 49–57, doi:10.1007/s00170-016-9719-5.
35. Chinchanikar, S.; Choudhury, S.K. Wear Behaviors of Single-Layer and Multi-Layer Coated Carbide Inserts in High Speed Machining of Hardened AISI 4340 Steel. *J MechSciTechnol***2013**, *27*, 1451–1459, doi:10.1007/s12206-013-0325-2.
36. Stachowiak, G.W. *Wear: Materials, Mechanisms and Practice*. Wiley: Chichester, England ; Hoboken, NJ, **2006**; pp. 191–220; ISBN 978-0-470-01628-2.